Crouzon Syndrome: Relationship of Rectus Muscle Pulley Location to Pattern Strabismus

Avery H. Weiss,[1,2] James Phillips,[1,3] and John P. Kelly[1,2]

[1]Roger Johnson Clinical Vision Laboratory, Division of Ophthalmology, Seattle Children's Hospital, Seattle, Washington
[2]Department of Ophthalmology, University of Washington Medical Center, Seattle, Washington
[3]Department of Otolaryngology, University of Washington Medical Center, Seattle, Washington

Correspondence: Avery H. Weiss, Division of Ophthalmology, OA.9.220, Seattle Children's Hospital, 4800 Sand Point Way NE, Seattle, WA 98105; avery.weiss@seattlechildrens.org.

Submitted: August 15, 2013
Accepted: December 2, 2013

Citation: Weiss AH, Phillips J, Kelly JP. Crouzon syndrome: relationship of rectus muscle pulley location to pattern strabismus. *Invest Ophthalmol Vis Sci*. 2014;55:310–317. DOI: 10.1167/iovs.13-13069

Purpose. Investigate the relationship between the extorsion of the rectus muscle pulleys and the V-pattern exotropia and "overelevation in adduction" observed in Crouzon syndrome.

Methods. Twenty children with Crouzon syndrome had assessment of eye alignment. The horizontal and vertical positions of the four rectus muscle pulleys were estimated from coronal CT images. Eye alignment was simulated in Orbit 1.8 software by shifting the corresponding location of the rectus muscle pulley array.

Results. Eleven of the 20 patients had a V-pattern exotropia with displacements of each rectus muscle pulley ranging from 2 to 7 mm. The remaining nine patients were orthotropic with <2 mm displacement of the rectus muscle pulleys. Simulated displacements (>2 mm) of either the horizontal or vertical rectus muscle pulleys produced a similar strabismus pattern. The amount of V-pattern exotropia observed clinically was highly correlated with the amount predicted by pulley displacements in Orbit 1.8 ($r^2 = 0.63$; $P < 0.0001$). The displacement of vertical and horizontal rectus muscle pairs was significantly higher for patients having overelevation in adduction.

Conclusions. Rotation of the four rectus muscle pulleys relative to the corresponding rotation planes of the globe changes the direction and magnitude of their active and passive pulling forces in a gaze-dependent manner. Extorsion of the horizontal and vertical rectus muscle pulleys in Orbit 1.8 reproduces the pattern strabismus observed in Crouzon syndrome. The high correlation between the predicted magnitude of the V-pattern exotropia and observed exotropia indicates that extorsion of the rectus muscle pulleys primarily accounts for the pattern strabismus.

Keywords: Crouzon syndrome, rectus muscle pulleys, craniofacial disorders

Crouzon syndrome is a genetic disorder characterized by generalized craniosynostoses (sutural fusion), maxillary hypoplasia, widely spaced (hypertelorism) but shallow orbits with prominent globes.[1] Premature closure of the coronal, sagittal, and lambdoidal sutures results in deformation of the head. Growth of the skull is increased in the plane of the fused suture but constrained in the plane perpendicular to the fused suture. Depending on the order and temporal progression of sutural closure, head shape can be elongated or foreshortened in the anteroposterior direction (scaphocephaly, brachycephaly) or expanded vertically (turricephaly). The head shape is typically brachycephalic in Crouzon syndrome. Abnormal head shape is usually obvious at birth and becomes more clinically apparent with increasing age. In a minority of cases with mild hypertelorism or subtle midface deficiency, the diagnosis may be delayed or go unrecognized. More than 50% of cases are genetic with autosomal dominant inheritance. Molecular studies have identified mutations of the fibroblast growth factor receptor 2 (FGFR2) in patients with Crouzon syndrome.[2–3]

Abnormalities of skull shape in Crouzon syndrome are associated with orbital dystopias that track with the associated bony deformities of the craniofacial skeleton. The resulting orbital dystopia frequently predisposes to ocular misalignment in Crouzon syndrome.[4–9] Horizontal and vertical strabismus has reported prevalences ranging from 33% to 86.6%.[10,11] Horizontal strabismus is characterized by exotropia or esotropia in central gaze and horizontal divergence in upgaze relative to downgaze, clinically referred to as an A-pattern or V-pattern. Vertical strabismus is characterized by overelevation of the adducting eye or excessive depression of the abducting eye in lateral gazes. Historically, the V-pattern exotropia was attributed originally to anomalies in the structure or insertion of extraocular muscles, posterior displacement, or absence of the superior and inferior oblique muscles and shallowness of the orbit.[10,11] The recent application of computed tomography (CT) and magnetic resonance imaging (MRI) revealed that the extraocular rectus muscles were extorted. Numerous investigators have proposed that extorsion of the rectus extraocular muscles leads to pulling forces orthogonal to their normally directed pulling force.[12–17] For example, lateral translation of the superior rectus muscle introduces a horizontal component to its pulling force that rotates each eye outward in upgaze. Likewise, medial translation of the inferior rectus muscle introduces a horizontal component to its pulling force that rotates each globe inward in downgaze.

In this study, we propose that CT or MRI evidence of extorsion of EOM and the pattern strabismus is directly linked to

TABLE. Clinical Findings in Crouzon Patients

Patient	Age/Sex	Visual Acuity RE	Visual Acuity LE	Central Gaze	Upgaze	Downgaze	OEA	Surgery
1	1.0/M	20/63	20/47	Ortho	Ortho	Ortho	None	CRA
2	1.5/M	20/100	20/80	Ortho	Ortho	Ortho	OU	None
3	1.6/M	20/190	20/190	Ortho	25XT	Ortho	OU	None
4	1.8/M	20/94	20/130	Ortho	Ortho	Ortho	OU	CRA × 2
5	2.8/M	20/60	20/70	65XT	80XT	35XT	OU	CRA
6	4.7/M	20/40	20/40	Ortho	18-20XT	Ortho	OU	CRA, MFA
7	5.1/F	20/30	20/25	20XT	40XT	Ortho	OU	CRA, MFA
8	5.3/F	20/200	2/400	45XT	40XT	65XT	OU	CRA
9	5.8/F	20/20	20/30	Ortho	Ortho	Ortho	None	None
10	6.0/F	20/20	20/20	Ortho	Ortho	Ortho	None	CRA, MFA
11	6.8/M	20/20	20/30	25XT	30XT	20XT	OU	CRA, MFA
12	7.3/M	20/20	20/20	Ortho	Ortho	Ortho	None	None
13	7.9/F	20/25	20/50	40XT, 12 RHT	65XT	Ortho	OU	CRA, MFA
14	9.3/F	20/20	20/30	30XT	45XT	Ortho	OU	CRA, MFA
15	9.8/F	20/25	20/25	Ortho	Ortho	Ortho	None	CRA, MFA
16	11.0/M	20/25	20/25	Ortho	4X	Ortho	None	CRA, MFA
17	11.9/M	20/20	20/20	Ortho	Ortho	Ortho	None	CRA ×2
18	11.9/M	20/30	20/30	25–30XT	65XT	Ortho	OU	CRA, MFA
19	12.2/F	20/70	20/100	30XT	50XT	0–20	OU	CRA, MFA
20	12.9/M	20/20	20/20	4X	12X	Ortho	None	None

CRA, craniotomy; LE, left eye; MFA, midface advancement; OEA, over-elevation adduction; Ortho, orthotropic; OU, both eyes; RE, right eye; RHT, right hypertropia; X, exophoria; XT, exotropia.

extorsion of the EOM pulleys. The present study had two aims. One aim was to quantify extorsion of the rectus muscle pulleys in Crouzon syndrome using CT imaging. A second aim was to simulate the CT-defined extorsion of the rectus muscle pulleys in ocular simulator software (Orbit 1.8; Eidactics, San Francisco, CA, provided in the public domain by http://eidactics.com) and to compare the eye alignment predicted by the model with clinical measurements of eye alignment.

METHODS

We prospectively studied 20 children with Crouzon syndrome after institutional review board approval was granted. The research adhered to the tenets of the Declaration of Helsinki. A pediatrician and plastic surgeon specializing in craniofacial disorders established the diagnosis in all patients. Crouzon syndrome was suspected on the basis of the variable presence of a misshapen skull, exorbitism, midface hypoplasia, and history of similarly affected relatives with autosomal dominant inheritance. In all cases, the craniofacial diagnosis was confirmed by CT documentation of premature closure of the coronal, sagittal, and lambdoidal sutures.

All of the patients had comprehensive eye examinations with emphasis on assessment of binocular eye alignment in central gaze and at eccentricities of 30° up, down, right, and left. Binocular alignment was quantified using the prism cover test or the Krimsky test depending upon patient cooperation. Stereopsis was measured in cooperative patients using the Titmus test. The eye examination was performed prior to craniofacial surgery or after craniofacial surgery. At surgery, an osteotomy is made 10 mm behind the superior orbital rim and the forehead is advanced anteriorly (fronto-orbital advancement) or the inferior orbital rim and anterior portion of the maxilla are advanced (midface advancement). Given that the rectus muscle pulleys are located at the posterior aspect of the globe (22–30 mm posterior to the orbital rim), we assume prior craniofacial surgery does not alter their location or anatomic function. One patient with hydrocephalus and comitant exotropia was excluded.

To model static eye alignment in central and eccentric gazes we used an ocular simulator software (Eidactics).[18,19] This program takes into account the passive and active forces exerted by each of the extraocular muscles along with the biomechanical properties of the ocular motor plant (orbit, muscle, connective tissues, and muscle pulleys). Eye position in central gaze and at 30° eccentricities in 5° steps is depicted on a Hess chart in Fick coordinates. The relationship between extorsion of the rectus muscle pulleys and either the V-pattern exotropia or "elevation in adduction" was then investigated in the ocular simulator software (Eidactics). This analysis was uniformly performed with the right eye fixing. The corresponding clinical measurements of horizontal eye alignment were primarily limited to central gaze and at eccentricities of 30° up and down. Because quantitation of the hypertropia in lateral gazes is problematic in this population, the corresponding clinical scoring of overelevation in adduction was limited to its presence or absence.

During the course of standard clinical care, all patients had a high-resolution CT of the head including the orbits using a 2-dimensional scanner (model CBTB-016A; Toshiba Corp., Tokyo, Japan, or Discovery STE; GE Medical Systems, Pewaukee, WI). The CT dose index (CTDI) was 22.73 or 34.91 for the initial study in children aged younger or older than 2 years, respectively. All subsequent studies were performed at a CTDI of one quarter to one-half of the initial dosage. Of note, this amount of radiation exposure is well below the threshold recommended by the American College of Radiology CTDI of 75 mGy. Patients' heads were stabilized using a foam cushion. Transaxial images of the head and maxillofacial skull were helically acquired using 2:1 pitch. Continuous axial images, 0.625 to 1.25 mm thick, were obtained using a 512 × 512 matrix covering a 24- by 24-cm square, giving a pixel resolution of 469 μm. CT images were exported in DICOM format to a Macintosh workstation, where they were analyzed quantitatively using imaging software (Osirix version 2.4; UCLA, Los Angeles, CA, provided in the public domain by http://www.osirix-viewer.com).[20] We selectively analyzed the CT images that were performed near the time of assessment of the corresponding eye alignment shown in the Table.

FIGURE 1. Axial CT scan from a patient with Crouzon syndrome showing a deflection along the axial paths of the horizontal rectus muscles that aligns with the back of the globe (*block arrows*).

CT image contrast was set to a bone window and subjectively increased or decreased to maximally distinguish the extraocular muscles from adjacent structures. The CT image volume was rotated using the 2-dimensional multiplanar reconstruction mode in the imaging software (UCLA) to coincide with the ocular simulator software (Eidactics) coordinates. The horizontal plane (defined by lateral-medial and anterior-posterior directions) was aligned with the inferior orbital rim and the external auditory canal, and the mid-points of the optic canals. The vertical plane (superior-inferior directions) was defined as orthogonal to this horizontal plane. To correct for rotation in the horizontal plane, we made sure that each optic canal was aligned with the horizontal axis on the axial CT image. Rotation of the horizontal plane was further confirmed in all patients by moving the CT image volume in the anterior direction and ensuring the posterior aspect of the globe was symmetric between the right and left side.

The relative horizontal position of the superior and inferior (SR/IR) and medial and lateral (MR/LR) rectus muscle pulleys were determined from coronal images normalized in the craniotopic coordinate system described previously. Measurements of the rectus muscle pulleys were taken within ±1.0 mm of the optic nerve/globe junction along the anterior-posterior axis of the image sections. Of note, this location is 6 mm behind the expected location of the rectus muscle pulleys which are normally 6 mm posterior to the center of the globe (Eidactics). Demer and collaborators[17,21–23] have shown that the pulley inflection is on average 6 mm posterior to the globe center in normal-sized eyes (total axial length = 24.5 mm) with normal orbital dimensions. We selected this location because in a subset of patients, this is where the globe was aligned with the deflection along the axial paths of the horizontal rectus muscles corresponding to the LR and MR pulleys (Fig. 1). The estimated pulley location was 12 mm ± 2 mm posterior to the center of the globe and consistent with the shallow orbit associated with Crouzon syndrome.

The position of each rectus muscle was measured using the technique described by Clark et al.[24] The coronal CT image at the estimated pulley location was exported to Java-based imaging software (ImageJ; National Institutes of Health, Bethesda, MD, provided in the public domain by http://rsbweb.nih.gov/ij/). Each rectus muscle, for each eye, was outlined in Java-based imaging software (NIH) and the central location of each rectus muscle was defined by the "area centroid" function. The ocular simulator software (Eidactics) defines the origin as the center of the globe when the eye muscles exert no force. The superior rectus pulley is opposite

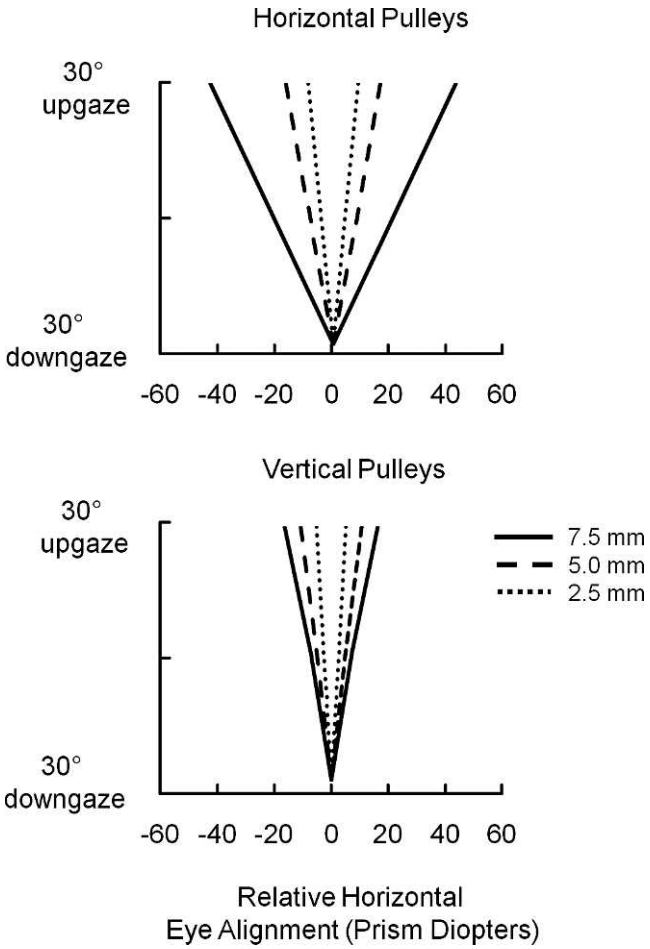

FIGURE 2. Predictions by the ocular simulator software (Eidactics) of V-pattern exotropia between 30 degrees downgaze and 30° upgaze following displacements of the SR/IR and MR/LR muscle pulleys of 2.5, 5.0, and 7.5 mm, respectively. Eye alignments (in prism diopters) are adjusted to be orthotropic at 30° downgaze by adding a constant vergence. *Top*: V-pattern exotropia predicted by symmetrical displacements of the medial and lateral rectus muscle pulleys. *Bottom*: V-pattern exotropia predicted by symmetrical displacements of the superior and inferior rectus muscle pulleys.

(180°) the inferior rectus pulley in the vertical plane and both are equidistant from the origin at the center of the globe. Likewise, the lateral rectus pulley is opposite (180°) from the medial rectus pulley in the horizontal plane and both are equidistant from the origin at the center of the globe. Since we cannot control the direction of gaze in young children undergoing a CT scan, we defined the origin as the intersection of all four recti muscles to fit the assumptions in the ocular simulator software (Eidactics). We then measured the relative horizontal and vertical offsets of the muscle center from their 180° relationships using the equations

$$\text{Horizontal displacement} = H*\cos(\alpha),$$

$$\text{Vertical displacement} = V*\sin(\alpha).$$

Where H is the distance from our origin to the nearest horizontal rectus muscle (lateral or medial), V is the distance from the origin to the nearest vertical rectus muscle (superior or inferior), and α is the angle of the relevant rectus muscle from the horizontal (or vertical) plane. These displacements were then used to adjust the corresponding rectus muscle

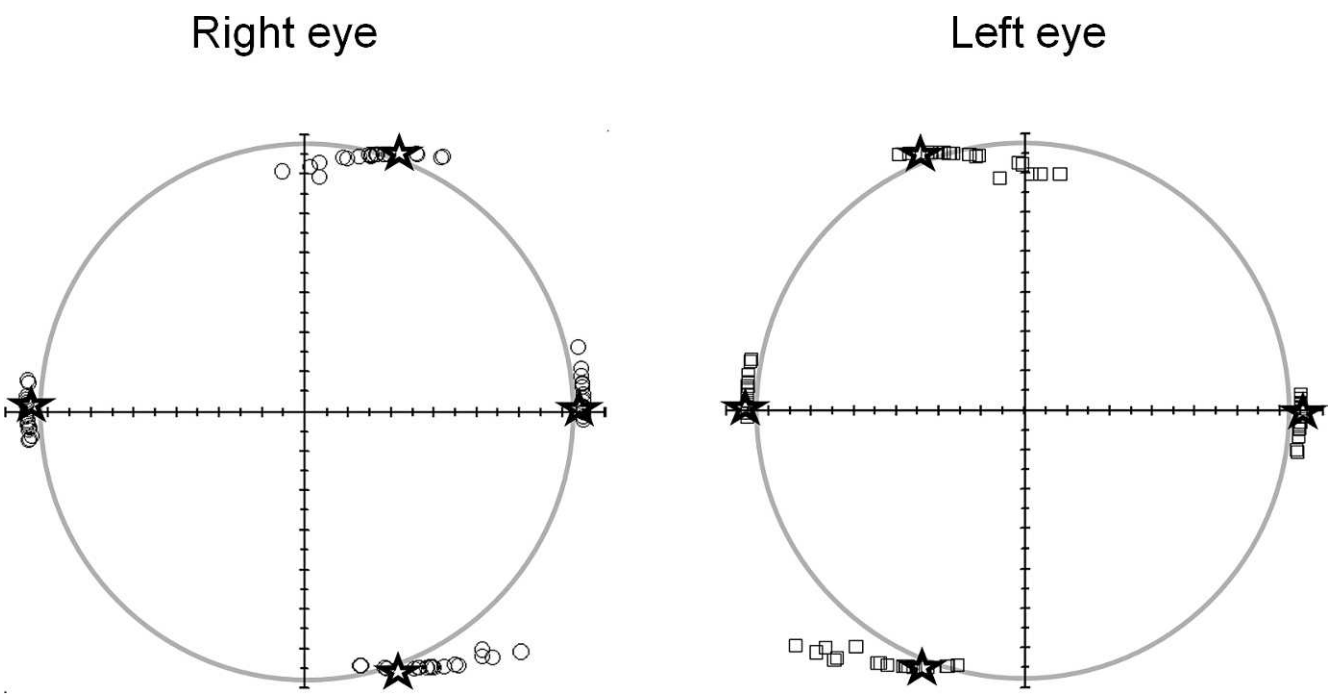

FIGURE 3. Anterior view of the central locations of the four rectus muscle pulleys relative to the globe. Each of the 20 patients is represented by *open symbols*. *Star symbols* indicate the normal pulley location for each rectus muscle. *Tick marks* on the axes represent 1 mm.

pulley in the ocular simulator software (Eidactics). All coordinates were adjusted for sign, which the ocular simulator software (Eidactics) defines positive directions from the origin as abduction, elevation, and extorsion. We then run the simulation and record the predicted eye alignment versus the observed clinical measurements.

RESULTS

The clinical characteristics of the 20 patients (12 males) are shown in the Table. Eleven (55%) of the 20 patients had a V-pattern exotropia. All patients with strabismus had CT evidence of extorsion (>2) mm of the horizontal rectus muscle pulleys, the vertical rectus muscle pulleys, or both. In comparison, none of the patients without strabismus had CT evidence of rectus muscle pulley extorsion. "Overelevation in adduction" was observed in each of the patients with a V-pattern strabismus but not in the orthotropic patients. Sixteen (80%) of the 20 had normal age-adjusted visual acuities bilaterally. Visual acuity was reduced due to optic atrophy secondary to increased intracranial pressure in three patients (patients 5, 8, and 19) and due to exposure keratopathy in patient 13. Fifteen of the 20 patients had craniotomies for expansion of the cranial vault; 10 had midface advancements. The five patients without previous surgery either had mild Crouzon ($n = 3$) or a predominant midface deformity ($n = 2$). In addition, three patients had a ventriculoperitoneal shunt for hydrocephalus due to an Arnold-Chiari malformation. Patients with comitant strabismus due to increased intracranial pressure were excluded from this study.

As proof of concept that extorsion of the rectus muscle pulleys can account for a V-pattern strabismus, we first simulated variable amounts of extorsion of the rectus muscle pulleys in the ocular simulator software (Eidactics). Figure 2 shows predicted eye alignment after by 2.5-, 5.0-, or 7.5-mm vertical offset of the horizontal rectus muscle pulleys and horizontal offsets of the vertical rectus muscle pulleys alone. The figure depicts a V-pattern with alternate fixation of either eye. Vertical offset of the medial rectus and lateral rectus muscle pulleys of 2.5, 5.0, and 7.5 mm produced a V-pattern exotropia that increases respectively from 17.4 to 32.8, and to 85.6 prism diopters. Of note, regression analysis of these data were fit by an exponential relationship ($y = 7.43e^{0.3186x}$; $r^2 = 1.0$). Horizontal offset of the superior rectus and inferior rectus muscle pulleys of 2.5, 5.0, and 7.5 mm produces a V-pattern exotropia that increases respectively from 10.4 to 21.6 and to 33.6 prism diopters. Of note, regression analysis of these data were fit by a linear relationship ($y = 4.52x - 0.9333$; $r^2 = 986$).

Figure 3 depicts the location of the four rectus muscle pulleys relative to the center of the globe from an anterior view. The symbol indicates the normal pulley locations in the ocular simulator software (Eidactics) for each rectus muscle. The location of each pulley across patients variably overlaps the cardinal axes. The distribution of the pulley locations relative to their normal location ranges from 0 to 5 mm for the medial rectus muscles, 0 to 5 mm for the lateral rectus muscles, 0 to 6 mm for the superior rectus muscles and 0 to 7 mm for the inferior rectus muscles. Despite the location differences across patients, opposing pulleys for individual patients are consistently located 180° apart and equidistant from the center of the globe. Of note, the geometry of the horizontal rectus muscle pulley locations is reliably fit by a circle because the distribution of the horizontal pulleys is tangential to the globe at its horizontal axis. In comparison, the vertical rectus muscle pulleys are not well fit by a circle because their linear distribution is displaced nasally and is not tangential to the globe.

Next, we compared the predicted impact of extorsion of the rectus muscle pulleys on binocular eye alignment with the clinical measurement in three patients. The location of each rectus muscle pulley was shifted both vertically and horizontally in the ocular simulator software (Eidactics) by an amount quantified by analysis of the corresponding CT images. Eye alignment for patients with 0 to 2°, 20°, and 32° of extorsion of the rectus muscle pulleys are shown as Hess-Lancaster–type plots in Figure 4. Eye position predicted by the ocular simulator

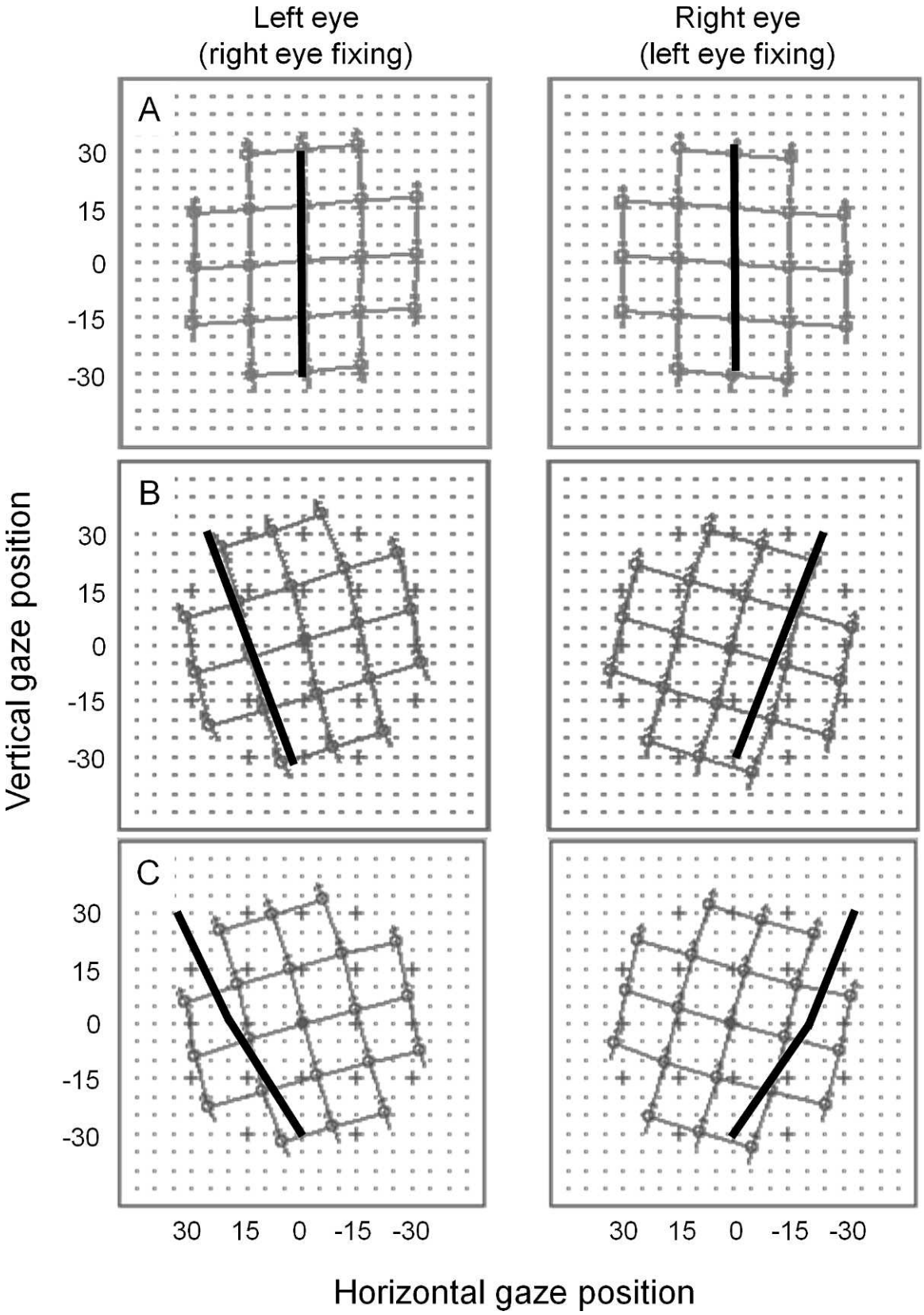

FIGURE 4. Hess-Lancaster–type plots of horizontal and vertical eye position predicted by the ocular simulator software (Eidactics) in three patients with Crouzon syndrome. (**A**) A patient with 0 to 2° extorsion; (**B**) A patient with 20° extorsion; and (**C**) A patient with 30° extorsion. Expected eye position is indicated by the *pluses* (+) and predicted eye position is indicated by *open circles* connected with *lines*. The observed clinical eye position is shown by *superimposed thick lines*. Plots on the left side are predictions for the left eye when the right eye is fixing. Plots on the right side are predictions for the right eye when the left eye is fixing. Positive vertical positions represent upgaze and positive horizontal positions represent adduction.

software (Eidactics) in central gaze and at eccentricities of 30° upgaze, downgaze, right gaze, and left gaze in 2.5 mm intervals is indicated by the circles. Eye position determined from clinical examination in central gaze and at eccentricities of 30° downgaze and 30° upgaze is represented by the pluses (+). Figure 4A shows the horizontal and vertical eye position in a patient without extorsion of the pulleys. The model predicted normal eye alignment in all gaze positions and the clinical examination showed normal eye alignment in all gaze positions. Figure 4B shows the horizontal and vertical eye position in a patient with 20° of extorsion of the pulleys. The model predicted a 16° V-pattern XT and the clinical examination showed a 20° V-pattern XT. Figure 4C shows the horizontal and vertical eye position in a patient with 32° of extorsion of the pulleys. The model predicted a 32° V-pattern XT and the clinical examination shows a 32.5° V-pattern exotropia. Of note, both Figures 4B and 4C showed that the simulation predicted a 15° esotropia in downgaze, whereas the clinical assessment showed binocular eye alignment in downgaze.

We then examined whether there was a relationship between the amount of V-pattern exotropia in central and eccentric gazes predicted by the model versus the amount measured on clinical examination. Vergence angle was adjusted to align the eyes in downgaze to account for patients with V-pattern exotropia. Figure 5 plots the predicted amount of exotropia on the *y*-axis versus the observed amount of exotropia on the *x*-axis as circles for each patient. The linear regression for all patients is depicted by the solid line. The linear regression was fit by a linear regression ($r^2 = 0.63$; $P = 0.00003$). Note the slope of this relationship is slightly less than 1.0. The subset of five outliers showing the most variability between predicted and observed eye alignment had pulley displacements of 0 to 2 mm. The five patients designated by filled circles did not have craniofacial surgery prior to assessment of the rectus muscle pulleys.

To explore the underlying basis of the overelevation in adduction observed in Crouzon syndrome, we analyzed the impact of torsion of the rectus muscle pulleys on vertical eye alignment. Figure 6 shows vertical eye alignment of the 20 patients in central gaze and at eccentricities of 30° right and left predicted by the ocular simulator software (Eidactics) with the right eye fixing. The location of each rectus muscle pulley for each patient was shifted vertically and horizontally by an amount determined from the corresponding CT images. The ocular simulator software (Eidactics) predicts that vertical alignment of the left eye can be hypertropic, orthotropic, or hypotropic in right gaze relative to left gaze. These findings are consistent with extorsion, absence of torsion, or intorsion of the globe, respectively. The ocular simulator software (Eidactics) predicted all but three patients had overelevation in adduction.

Figure 7 shows the distributions of torsion (mean ± 2 SD) of the vertical rectus and the horizontal rectus muscle pulleys with overelevation in adduction (upper and lower graphs, respectively). For the vertical rectus muscle pulleys, the mean (±SD) extorsion was −12.0° (±10.3) and −2.0° (±6.3) for patients with or without overelevation in adduction, respectively. For the horizontal rectus muscle pulleys, the mean extorsion was −4.4 (±3.9) and −1.1° (±2.4) for patients with or without overelevation in adduction, respectively. The differences in the distributions for the vertical and horizontal rectus muscle pulleys were significant (*t*-test, $P = 0.0005$; $P = 0.002$, respectively).

Discussion

In this study, we show that extorsion of the rectus muscle pulleys is highly correlated with extorsion of the globes, V-pattern exotropia, and "overelevation in adduction" associated with Crouzon syndrome. As proof of concept, we documented that selective upward/downward translation of the MR/LR muscle pulleys (2.5-, 5.0-, and 7.5-mm) and medial/lateral translation of the SR/IR muscle pulleys (2.5-, 5.0-, and 7.5-mm) in a biomechanical model of eye alignment reproduces a V-pattern exotropia and overelevation in adduction. We then show that alignment predicted by the simulator software (Eidactics) after adjustment for the measured horizontal and vertical translation of the rectus muscle pulleys in three patients' overlaps observed eye alignment (Fig. 4). Finally, we show for all patients that observed exotropia is strongly correlated with the exotropia predicted from translation of the rectus muscle pulleys. In contrast, anterior/posterior translation of the rectus muscle pulleys to simulate the shallow orbits in Crouzon syndrome did not result in extorsion of the globe or strabismus. Furthermore, the patient subset with normal pulley locations and shallow orbits did not demonstrate the pattern strabismus or overelevation in adduction.

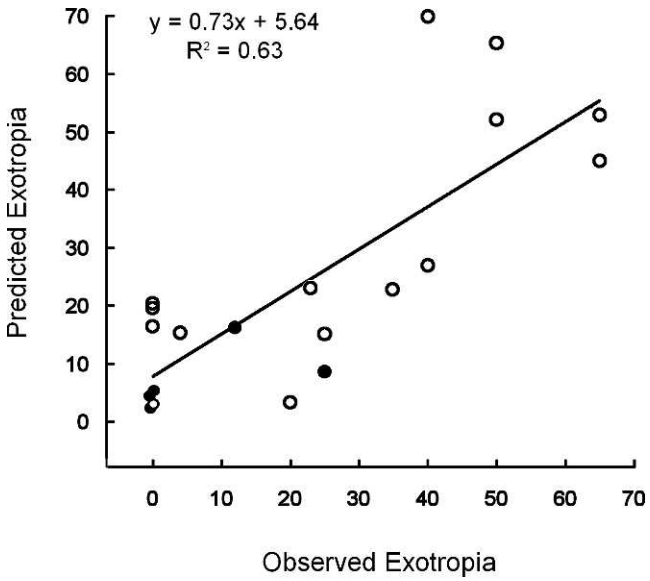

Figure 5. Relationship between the amount of V-pattern exotropia predicted by the ocular simulator software (Eidactics) and the amount of V-pattern exotropia observed clinically.

We demonstrated that the rectus muscle pulleys were variably translated in Crouzon syndrome. Some patients showed no or minimal displacements while others showed up to 7 mm of translation. Although the range of EOM pulley displacements is relatively small, they are substantial when summed together and normalized to the circumference of a normal-sized globe (75.3 mm). The finding that opposing rectus muscle pulleys are collinear despite their displacement suggests that the gaze-dependent alterations in eye alignment can still be modeled by a combination of their active pulling direction and passive pulling forces. The presence of noncollinear alignment of rectus muscle pairs would impose complex, off-axis, pulling forces.

Extorsion of the rectus muscle pulleys results in gaze-dependent alterations in the passive pulling forces of paired SR/IR and MR/LR muscles of each eye. The passive pulling force of the superior rectus muscles exceeds that of the inferior rectus muscle in contralateral gaze owing to its increased stretch. Conversely, the passive pulling force of the inferior rectus muscles exceeds that of the superior rectus muscles in ipsilateral gaze where it is on greater stretch. For the horizontal rectus muscles, the passive pulling force of the

Investigative Ophthalmology & Visual Science

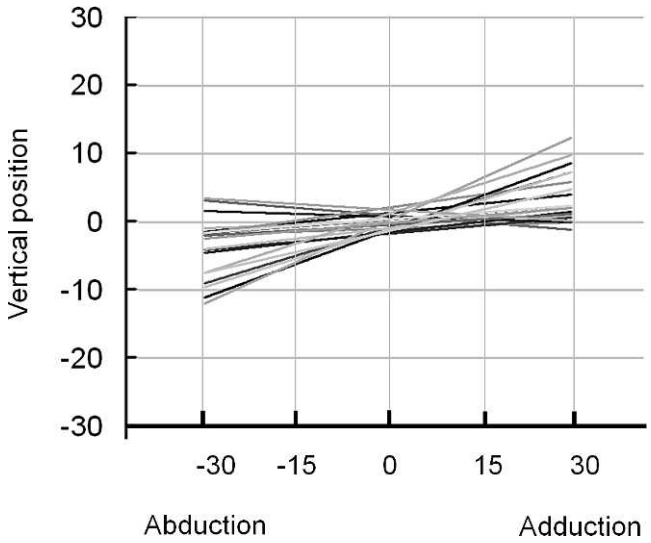

FIGURE 6. Change in vertical position of the left eye relative to the fixating right eye with positive values indicating hypertropia and negative values hypotropia. Data for 20 patients were predicted from the ocular simulator software (Eidactics) for central gaze, 30° abduction and 30° adduction.

lateral rectus muscles exceeds that of the medial rectus muscles in upgaze owing to its increased stretch. Conversely, the relative pulling force of the medial rectus muscles exceeds that of the lateral rectus muscles in downgaze where the medial recti are stretched more than the lateral recti.

Extorsion of the SR/IR and LR/MR rectus muscle pulley pairs relative to the corresponding rotation planes of the globe also changes their pulling direction. The pulling direction of each rectus EOM is defined by its anterior path, which functionally originates at the muscle pulley and terminates at the tendinous muscle insertion. Lateral translation of the superior rectus muscle pulleys combined with medial translation of the inferior rectus muscle pulleys creates an angular misalignment in their pulling direction relative to the vertical rotation plane of the globe. Similarly upward translation of the medial rectus muscle and downward translation of the lateral rectus muscle pulleys creates an angular misalignment in their pulling direction relative to the horizontal rotation plane of the globe. As a consequence of these angular misalignments, the direction of their active pulling forces shift from either the vertical or horizontal axes to oblique axes. The horizontal component of the superior rectus now pulls each eye outwards in upgaze and that of the inferior rectus muscle pulls each eye inwards in downgaze, resulting in a V-pattern strabismus. Likewise, the vertical component of the lateral rectus muscle now pulls the abducting eye downward and the vertical component of the medial rectus muscle pulls the adducting eye upward in lateral gazes, producing vertical divergence.

Because the anatomic configuration of corresponding rectus muscles of the two eyes are a mirror image, the active and passive pulling forces of muscle pairs will add thereby increasing the V-pattern strabismus and the vertical divergence in lateral gaze. Over the range of observed displacements of rectus muscle pulleys, the ocular simulator software (Eidactics) predicts linear increases for offsets of the SR/IR muscle pulleys and nonlinear increases for offsets of the MR/LR muscle pulleys. In other words, the pulling force due to muscle stretch disproportionately increases exceeding that of the corresponding active pulling force.

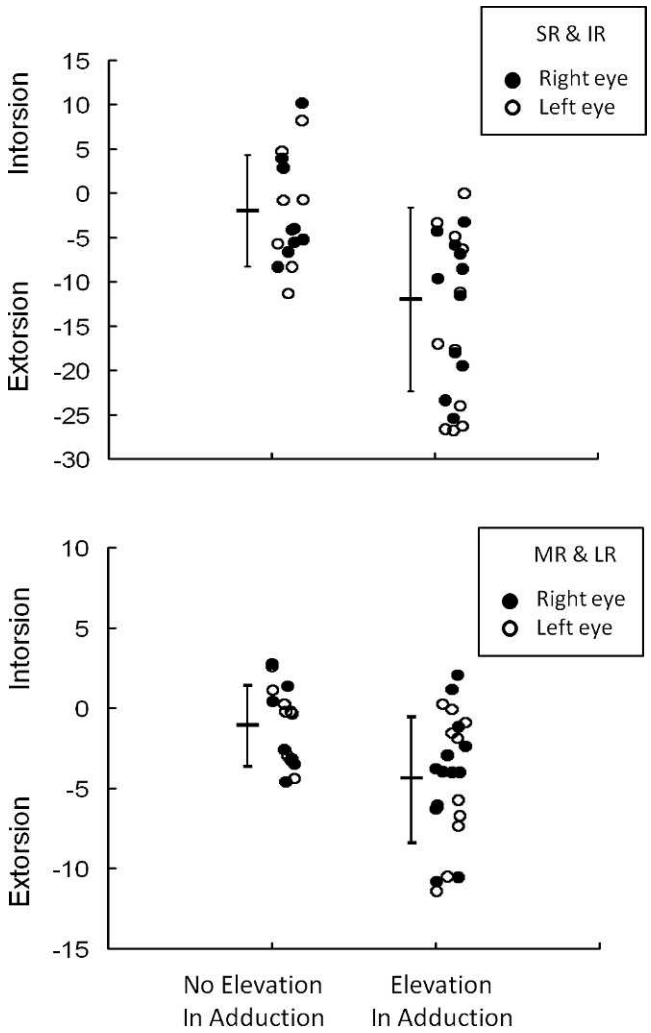

FIGURE 7. Distributions of globe torsion represented in degrees with positive values indicating intorsion and negative values extorsion are shown for patients with and without clinical evidence of overelevation in adduction. The *upper* and *lower graphs* show the corresponding contribution of the vertical and horizontal rectus muscle pulleys to the overall torsion of the globe. The *vertical bars* represent the values for the mean ± 2 SD.

The discrepancy between the fit of the ocular simulator software (Eidactics) model and the clinical data suggests that divergence is added to the relative balance of opposing active and passive muscle forces moving the position of alignment to 30° downgaze. At all other gaze positions, there is a superimposed V-pattern exotropia with vertical divergence. There is at least one potential advantage of the shift in the alignment point from central gaze to 30° downgaze. In V-pattern exotropia, the relative areal extent of the monocular visual representation of each eye is increased, whereas that of the rivalrous, binocular visual representation is decreased. In X-pattern exotropia, the relative areal extent of the monocular visual representation of each eye is decreased, whereas the area of rivalrous, binocular visual representation is increased.

Lastly, we considered additional factors that may account for the remaining variance in the relationship between the predicted and observed amount of V-pattern exotropia. Previously, Clark et al.[17] have shown that displacements of the rectus muscle pulleys can produce an incomitant strabismus that mimics oblique muscle dysfunction. Therefore,

primary overaction of the inferior oblique cannot be categorically implicated in the V-pattern strabismus in Crouzon syndrome. However, owing to the inability of CT imaging to adequately visualize the inferior oblique muscle, we were unable to characterize its potential contribution to globe extorsion. Future studies using MRI to assess oblique muscle function will likely provide further insight into the relative contribution of the inferior oblique to the V-pattern strabismus.[25] A second possibility is the potential impact of craniofacial surgery on the positional alignment of the rectus muscle pulleys. Presently, this surgery is performed before 2 years of age to prevent constraint of brain growth and craniofacial disfigurement. Surgically, the fronto-orbital advancement includes an osteotomy of the sphenoid wing 10 mm posterior to the superior orbital rim. Although this incision is 12 to 20 mm anterior to the horizontal rectus muscle pulleys, we cannot exclude the possibility of a remote translational effect on the rectus muscle pulleys during postnatal growth.

Acknowledgments

Preliminary results from this study were presented at the annual meeting for the Association for Research in Vision and Ophthalmology, Seattle, Washington, May 2013.

Supported by an unrestricted grant from the Peter LeHaye, Barbara Anderson, and William O. Rogers endowment funds. The authors alone are responsible for the content and writing of the paper.

Disclosure: **A.H. Weiss**, None; **J. Phillips**, None; **J.P. Kelly**, None

References

1. Cohen MM Jr, MacLean RE. *Craniosynostosis: Diagnosis, Evaluation and Management*. New York, NY: Oxford University Press; 2000:158–174.
2. Reardon W, Winter RM, Rutland P, Pulleyn LJ, Jones BM, Malcolm S. Mutations in the fibroblast growth factor receptor 2 gene cause Crouzon syndrome. *Nat Genet*. 1994;8:98–103.
3. Jabs EW, Li X, Scott AF, et al. Jackson-Weiss and Crouzon syndromes are allelic with mutations in fibroblast growth factor receptor 2. *Nat Genet*. 1994;8:275–279.
4. Miller MT. Ocular abnormalities in craniofacial malformations. *Int Ophthalmol Clin*. 1984;24:143–163.
5. Morax S. Oculo-motor disorders in craniofacial malformations. *J Maxillofac Surg*. 1984;12:1–10.
6. Carruthers JD. Strabismus in craniofacial dysostosis. *Graefes Arch Clin Exp Ophthalmol*. 1988;226:230–234.
7. Fries PD, Katowitz JA. Congenital craniofacial anomalies of ophthalmic importance. *Surv Ophthalmol*. 1990;35:87–119.
8. Coats DK, Paysse EA, Stager DR. Surgical management of V-pattern strabismus and oblique dysfunction in craniofacial dysostosis. *J AAPOS*. 2000;4:338–342.
9. Gobin MH. Sagittalization of the oblique muscles as a possible cause for the "A", "V", and "X" phenomena. *Br J Ophthalmol*. 1968;52:13–18.
10. Diamond GR, Katowitz JA, Whitaker LA, Quinn GE, Schaffer DB. Variations in extraocular muscle number and structure in craniofacial dysostosis. *Am J Ophthalmol*. 1980;90:416–418.
11. Morax S, Pascal D, Barraco P. Significance of the "V" syndrome with double "up shoot". Insufficiency of the two superior oblique muscles in craniofacial malformations. *J Fr Ophtalmol*. 1983;6:295–310.
12. Caputo AR, Lingua RW. Aberrant muscular insertions in Crouzon's disease. *J Pediatr Ophthalmol Strabismus*. 1980; 17:239–241.
13. Saunders RA, Holgate RC. Rectus muscle position in V-pattern strabismus. A study with coronal computed tomography scanning. *Graefes Arch Clin Exp Ophthalmol*. 1988;226: 183–186.
14. Cheng H, Burdon MA, Shun-Shin GA, Czypionka S. Dissociated eye movements in craniosynostosis: a hypothesis revived. *Br J Ophthalmol*. 1993;77:563–568.
15. Clark RA, Miller JM, Rosenbaum AL, Demer JL. Heterotopic muscle pulleys or oblique muscle dysfunction? *J AAPOS*. 1998; 2:17–25.
16. Tan K, Sargent M, Poskitt K, Lyons C. Ocular overelevation in adduction in craniosynostosis: is it the result of excyclorotation of the extraocular muscles? *J AAPOS*. 2005;9:550–557.
17. Clark RA, Demer JL. Magnetic resonance imaging of the effects of horizontal rectus extraocular muscle surgery on pulley and globe positions and stability. *Invest Ophthalmol Vis Sci*. 2006; 47:188–194.
18. Robinson DA. A quantitative analysis of extraocular muscle cooperation and squint. *Invest Ophthalmol*. 1975;14:801–825.
19. Miller JM, Robinson DA. A model of the mechanics of binocular alignment. *Comput Biomed Res*. 1984;17:436–470.
20. Rosset A, Spadola L, Ratib O. OsiriX: an open-source software for navigating in multidimensional DICOM images. *J Digit Imag*. 2004;17:205–216.
21. Demer JL, Miller JM, Poukens V, Vinters HV, Glasgow BJ. Evidence for fibromuscular pulleys of the recti extraocular muscles. *Invest Ophthalmol Vis Sci*. 1995;36:1125–1136.
22. Kono R, Poukens V, Demer JL. Quantitative analysis of the structure of the human extraocular muscle pulley system. *Invest Ophthalmol Vis Sci*. 2002;43:2923–2932.
23. Miller JM, Demer JL, Poukens V, Pavlovski DS, Nguyen HN, Rossi EA. Extraocular connective tissue architecture. *J Vis*. 2003;3:240–251.
24. Clark RA, Miller JM, Demer JL. Three-dimensional location of human rectus pulleys by path inflections in secondary gaze positions. *Invest Ophthalmol Vis Sci*. 2000;41:3787–3797.
25. Kono R, Demer JL. Magnetic resonance imaging of the functional anatomy of the inferior oblique muscle in superior oblique palsy. *Ophthalmology*. 2003;110:1219–1229.

Investigative Ophthalmology & Visual Science